THE JOURNAL OF PHYSICAL CHEMISTRY A

ARTICLE

pubs.acs.org/JPCA

Thermal Decomposition Mechanism of 1-Ethyl-3-methylimidazolium Bromide Ionic Liquid

Steven D. Chambreau,[†] Jerry A. Boatz,[‡] Ghanshyam L. Vaghjiani,[*,‡] Christine Koh,[§] Oleg Kostko,[∥] Amir Golan,[∥] and Stephen R. Leone[§,∥]

[†]ERC, Inc., Edwards Air Force Base, California 93524, United States

[‡]Propellants Branch, Propulsion Directorate, Air Force Research Laboratory, AFRL/RZSP, Edwards Air Force Base, California 93524, United States

[§]Departments of Chemistry and Physics, University of California, Berkeley, California 94720, United States

[∥]Lawrence Berkeley National Laboratory, Berkeley, California 94720, United States

ABSTRACT: In order to better understand the volatilization process for ionic liquids, the vapor evolved from heating the ionic liquid 1-ethyl-3-methylimidazolium bromide ($EMIM^+Br^-$) was analyzed via tunable vacuum ultraviolet photoionization time-of-flight mass spectrometry (VUV-PI-TOFMS) and thermogravimetric analysis mass spectrometry (TGA-MS). For this ionic liquid, the experimental results indicate that vaporization takes place via the evolution of alkyl bromides and alkylimidazoles, presumably through alkyl abstraction via an S_N2 type mechanism, and that vaporization of intact ion pairs or the formation of carbenes is negligible. Activation enthalpies for the formation of the methyl and ethyl bromides were evaluated experimentally, $\Delta H^{\ddagger}(CH_3Br) = 116.1 \pm 6.6$ kJ/mol and $\Delta H^{\ddagger}(CH_3CH_2Br) = 122.9 \pm 7.2$ kJ/mol, and the results are found to be in agreement with calculated values for the S_N2 reactions. Comparisons of product photoionization efficiency (PIE) curves with literature data are in good agreement, and *ab initio* thermodynamics calculations are presented as further evidence for the proposed thermal decomposition mechanism. Estimates for the enthalpy of vaporization of $EMIM^+Br^-$ and, by comparison, 1-butyl-3-methylimidazolium bromide ($BMIM^+Br^-$) from molecular dynamics calculations and their gas phase enthalpies of formation obtained by G4 calculations yield estimates for the ionic liquids' enthalpies of formation in the liquid phase: $\Delta H_{vap}(298\ K)$ $(EMIM^+Br^-) = 168 \pm 20$ kJ/mol, $\Delta H_{f,\ gas}(298\ K)$ $(EMIM^+Br^-) = 38.4 \pm 10$ kJ/mol, $\Delta H_{f,\ liq}(298\ K)$ $(EMIM^+Br^-) = -130 \pm 22$ kJ/mol, $\Delta H_{f,\ gas}(298\ K)$ $(BMIM^+Br^-) = -5.6 \pm 10$ kJ/mol, and $\Delta H_{f,\ liq}(298\ K)$ $(BMIM^+Br^-) = -180 \pm 20$ kJ/mol.

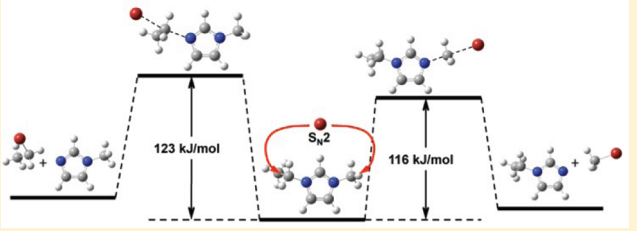

INTRODUCTION

Recent interest in ionic liquids, salts with melting points less than or equal to 100 °C, has stemmed from their extremely low volatility, thermal stability, and the enormous number of ionic liquids possible ($\sim 10^{18}$)[1] by varying either the cation or the anion. The physical and chemical properties of ionic liquids can also be tailored by modifying the functional groups on either ion. Ionic liquids have been studied for use as replacement solvents for volatile organic compounds (VOCs),[2−5] fuel cells,[6−9] electrolytes,[10,11] ingredients for energetic materials and propellants,[12−14] and as high-temperature lubricants.[15−17]

Understanding thermal stability of ionic liquids is important for the safe storage and transportation of these compounds.[18] Protic ionic liquids, having a hydrogen bound to a nitrogen on the cation, are thermally unstable and easily neutralized via proton transfer to the anion.[19] These neutral species can volatilize and reform ionic liquids on co-condensation of the vapors by the acid−base reaction. Aprotic imidazolium ionic liquids, having alkylated nitrogens in the cation, have been seen to undergo dealkylation under pyrolytic conditions to yield 1-substituted imidazoles, presumably through an S_N2 type mechanism,[18,20−22] which would explain why the thermal stability of imidazolium-based ionic liquids increases with increasing anion size,[20,23] increasing the length of the side chain (steric effects),[20] or decreasing nucleophilicity of the anion.[20] Alkyl substituents such as vinyl and phenyl tend to increase the stability of the cation due to charge delocalization to the side chain and are not susceptible to cleavage,[20] while secondary and tertiary alkyl groups on the cation make the ionic liquid less thermally stable, presumably due to the elimination of the stabilized alkyl cations.[24] There is also some evidence for the elimination of ethylene from ethylimidazolium ionic liquids with increasing basicity of the anion.[20] The acidic character of the C2 proton of the imidazolium cation, illustrated by the facile deuterium

Special Issue: A. R. Ravishankara Festschrift

Received: September 28, 2011
Revised: November 17, 2011
Published: November 18, 2011

exchange in D_2O,[25] seen also in thiazolium salts,[26] could also be a factor in the thermal stability of imidazolium-based ionic liquids, and addition reactions with the imidazolium ring have been observed at high temperatures.[22] Alkyl substitution of the C2 hydrogen on the imidazolium ring has the largest effect on the thermal stability due to the acidity of this proton.[24] This acidity stems from the stability of the carbene species formed upon proton loss from C2.[25,27] This n-heterocyclic carbene (NHC) species may play an important role in the addition reactions mentioned above,[28−30] and its formation can be facilitated by basic anions.[31] While the presence of oxygen does not appear to affect the temperature of decomposition of imidazolium ionic liquids, ionic liquids having endothermic decompositions in an inert atmosphere turn exothermic in an oxygen atmosphere midway through the observed mass loss in thermogravimetric analysis (TGA) when combustion dominates.[24]

Previous studies on the vaporization of ionic liquids indicate that some aprotic ionic liquids, especially those with anions that are the conjugate bases of superacids,[32] vaporize as intact ion pairs, evidenced by the frequent dissociative ionization of the ion pair and the detection of the intact cation by mass spectrometry: $C^+A^- + h\nu \rightarrow C^+A + e^- \rightarrow C^+ + A\cdot + e^-$. The removal of the electron from the anion eliminates the Coulombic attraction between the ions, and the weakly bound cation-radical complex dissociates prior to detection in the mass spectrometer. Direct detection of the ion pair via mass spectrometric techniques has been elusive, but recent progress has been made to directly identify these in the gas phase, including pulsed field ionization[33] and vacuum ultraviolet photoionization time-of-flight mass spectrometry (VUV-PI-TOFMS).[34]

If the rates of thermal decomposition of ionic liquids are comparable to the rate of evaporation of ion pairs from the ionic liquid, the resulting species in the gas phase are a mixture of thermal decomposition products and vaporized ion pairs. Effusive sources of ionic liquid vapors[35−38] impart substantial internal energy to the ion pair upon vaporization, which can facilitate dissociation.

In this paper, a combination of mass spectrometric techniques is used to evaluate the gas phase decomposition products upon heating the aprotic ionic liquid, 1-ethyl-3-methylimidazolium bromide ($EMIM^+Br^-$). The high sensitivity of VUV PI-TOFMS enables the detection of thermal decomposition products well below the thermal decomposition onset temperature determined via differential scanning calorimetry (DSC) and TGA. The results from the TGA-MS experiments complement the VUV-PI-TOFMS data and give a better understanding of the underlying processes and chemistry involved when heating $EMIM^+Br^-$. Accompanying ab initio calculations support the proposed decomposition mechanism by enabling the determination of possible photoion fragmentation pathways and gas phase enthalpies of formation. The calculated gas phase enthalpies of formation in conjunction with enthalpies of vaporization determined by molecular dynamics (MD) simulations allow for estimation of enthalpies of formation of ionic liquids in the liquid phase, a valuable but difficult to determine property of ionic liquids. Enthalpy of vaporization and enthalpy of formation values determined here are consistent with previously reported values for $BMIM^+Br^-$[39] and further support this thermal decomposition mechanism.

EXPERIMENTAL SECTION

$EMIM^+Br^-$ was purchased from Fluka (certified purity = 99.6%, water = 0.27%), and was used without further purification. DSC measurements were carried out on a TA Instruments DSC 2010 apparatus with a typical sample mass of 5 mg at a heating rate of 2 K/min in sealed aluminum pans with a nitrogen flow rate of 20 mL/min. The reference sample was an empty Al container, which was sealed under nitrogen atmosphere. Temperatures are determined to ±1 K with a previously calibrated thermocouple.

TGA-MS was carried out on a TA Instruments Q500 apparatus with an electron impact ionization energy of 70 eV. An ionic liquid sample of approximately 5 mg was analyzed under N_2 (10 mL/min) at 473 K for 1 h, followed by increasing the temperature at a rate of 5 K/min up to 643 K. The capillary tube between the TGA unit and the mass spectrometer was held constant at 473 K.

The VUV-PI-TOFMS experiments were performed at the Chemical Dynamics beamline 9.0.2.3 at the Advanced Light Source synchrotron facility at the Lawrence Berkeley National Laboratory, Berkeley, CA. Details of the experiment and the effusive source have been described previously.[35,36] Briefly, photoionization mass spectra were measured from 8.0 to 15.0 eV in 0.1 eV steps at 457 K. At each energy, the spectrum was averaged over 500 000 pulses of the ion repeller.

Ab initio calculations were carried out at the DFT (utilizing the B3LYP[40−42] and M06[43] functionals), MP2, and CCSD(T) levels of theory using the 6-31+G(d,p) basis set.[44−48] Enthalpies of activation and reaction were refined at the M06 and CCSD(T) levels with the more flexible augmented correlation-consistent polarized valence triple-ζ (aug-cc-pvtz) basis set.[49,50] All MP2 and CCSD(T) calculations described above were performed using GAMESS,[51,52] and the DFT computations were performed using Gaussian09.[53] Furthermore, gas phase enthalpies of formation of selected species were computed at the G4[54] level of theory using Gaussian09.[53] All calculated results are at 298 K and include zero point vibrational energy (ZPVE) corrections, unless otherwise stated. While B3LYP did not provide sufficient accuracy for these systems, MP2 and M06 methods provided accurate results when compared to similar bromine-containing species with known enthalpies of formation. M06 resulted in comparable accuracy to MP2 for these systems with significantly reduced computational cost.

MD simulations were performed using a polarizable force field, APPLE&P,[55] which was extended to include a description of the Br anion. MD simulations of bulk $BMIM^+Br^-$ and $EMIM^+Br^-$ ILs have been conducted at the desired temperatures and at atmospheric pressure. Each system contained 150 ionic pairs. MD simulations were conducted using the molecular simulation package Lucretius,[56] which has the capability to handle polarization effects. Covalent bond lengths were constrained using the velocity-Verlet form of the SHAKE algorithm.[57] The Ewald summation method was used for treatment of long-range electrostatic forces between partial atomic charges and between partial charges and induced dipoles. A tapering function was used to drive the induced dipole/induced dipole interactions to zero at the cutoff of 10 Å, with scaling starting at 9.3 Å. Induced dipoles were calculated via a direct iteration with a predictor corrector method. A cutoff of 10 Å was used for all van der Waals interactions and the real part of electrostatic interactions in the Ewald summation. A multiple time step reversible reference system propagator algorithm[58] was employed. A time step of 0.5 fs was used for bonding, bending, dihedral, and out-of-plane deformation motions, while a 1.5 fs time step was used for nonbonded interactions within cutoff radius of 6.0 Å. Finally, the nonbonded interactions in the range between 6.0 and 10.0 Å and reciprocal

part of electrostatic interactions were updated every 3 fs. Each system was initially equilibrated in the NPT ensemble for at least 1 ns, while production runs were over 5 ns. To calculate the enthalpy of vaporization, an ensemble of 150 ion pairs in the gas phase has been simulated using Brownian dynamics simulations. In these simulations, ions in a given (predefined) pair were allowed to interact only with each other, while any interactions with other ion pairs were turned off. All nonbonded interactions (van der Waals and electrostatic) were directly calculated for all possible pairwise interactions without any cutoff radius. Polarization effects were calculated taking into account only the electrostatic field created by the ionic pair. The duration of these simulations was over 1 ns allowing accurate sampling of the total energy per ion pair in the gas phase.

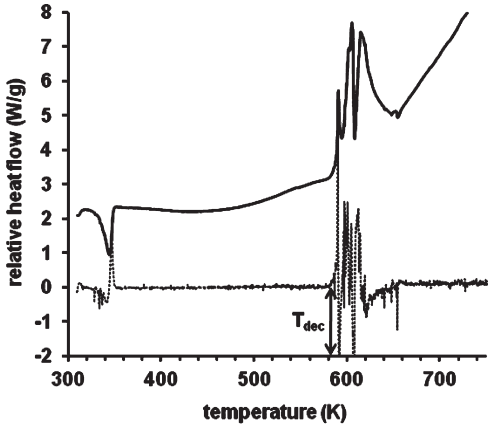

Figure 1. DSC curve for $EMIM^+Br^-$ ionic liquid (solid line). Dotted line is the slope of the DSC curve. T_{dec} = 585 K.

RESULTS

DSC. In order to evaluate the thermal decomposition onset temperature for the ionic liquid in this study, DSC was carried out (Figure 1). For $EMIM^+Br^-$ in Figure 1, melting occurs between 320 and 340 K, which is slightly lower than the literature value (349.9 K),[59] and this melting point depression is likely due to impurities and a small amount of absorbed water present. The decomposition is exothermic, indicated by a positive peak from 585 to 640 K. The jagged features in the DSC curve are probably a result of the sealed aluminum sample holder bursting from the increase in pressure upon decomposition; this feature was reproducible even with very small samples, and damage to the DSC sample containers was observed after the experiments. The onset thermal decomposition temperature, T_{dec}, for $EMIM^+Br^-$, reported as the initial nonzero slope of the DSC curves, is 585 K, which is in good agreement with previous TGA results (T_{dec} = 584 K).[24] It should be noted that for the VUV-PI-TOFMS experiments, temperatures well below this apparent onset decomposition temperature were chosen to look for possible vaporization of the ionic liquid (T = 457, 510, 560 K). However, the slight increase in the DSC heating curve beginning at around 450 K could indicate that a small amount of thermal decomposition occurs well below T_{dec}.

TGA-MS. In an effort to understand the gas phase species evolved from the heated ionic liquid as a function of temperature, TGA-MS measurements were performed. Typical results for $EMIM^+Br^-$ are presented in Figure 2. In Figure 2a, the major product peaks detected are at m/z 94($CH_3{}^{79}Br$), 96($CH_3{}^{81}Br$), 108($CH_3CH_2{}^{79}Br$), and 110($CH_3CH_2{}^{81}Br$), and their temperature profiles can be seen in Figure 2b. These masses are seen at all temperatures (473−643 K). Their relative mass intensities do not change significantly with increasing temperature, indicating that thermal decomposition occurs even at 473 K, which is well

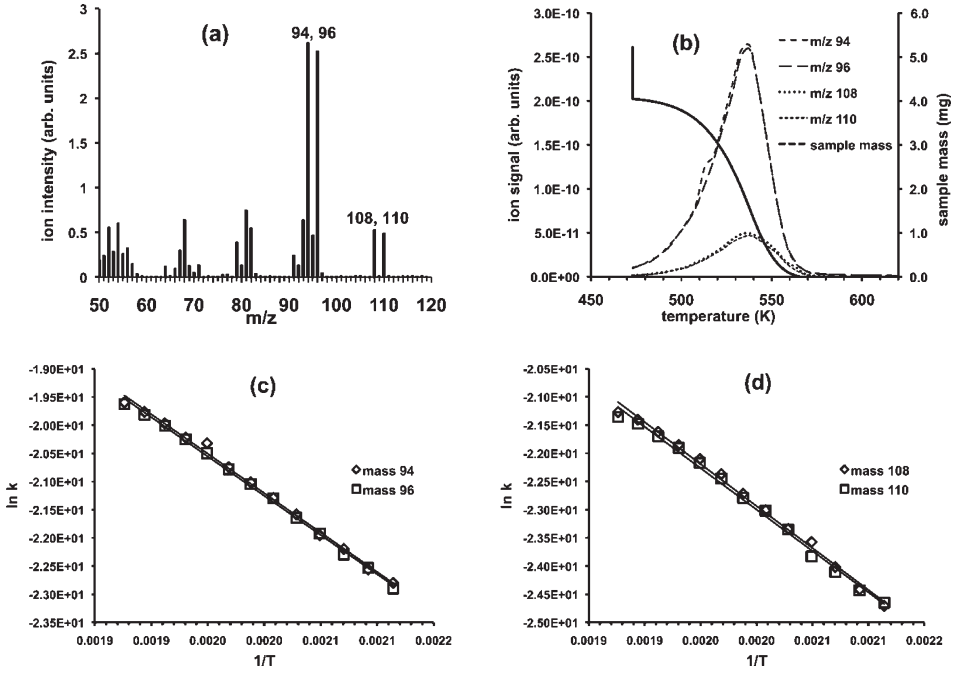

Figure 2. (a) TGA-MS data of $EMIM^+Br^-$ averaged over 60 min at 473 K. (b) TGA-MS data of $EMIM^+Br^-$ and for m/z 94, 96, 108, and 110 as a function of temperature. The isotherm at 473 K is represented by the vertical solid line. (c) Arrhenius plot for determination of $\Delta H^{\ddagger}$ for the formation of CH_3Br. (d) Arrhenius plot for determination of $\Delta H^{\ddagger}$ for the formation of C_2H_5Br.

dx.doi.org/10.1021/jp209389d |J. Phys. Chem. A 2012, 116, 5867–5876

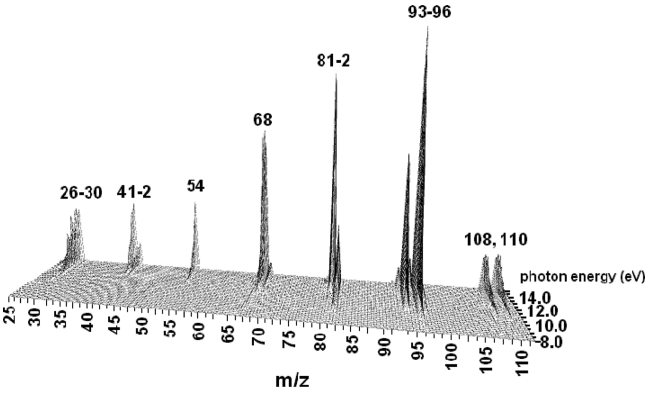

Figure 3. VUV-PI-TOFMS results for heated $EMIM^+Br^-$ ionic liquid in an effusive source, with source temperature T = 457 K. Photoion AEs are listed in Table 1.

Table 1. VUV Photoion AEs (in eV, ±0.2 eV) for the Gaseous Products When $EMIM^+Br^-$ Is Heated to 457 K

m/z	41	42	54	68	81	82	94	96	108	110
AE	12.7	12.0	11.9	10.9	11.1	8.6	10.5	8.5	10.3	10.3

below the thermal decomposition onset temperature indicated in the DSC (T_{dec} = 585 K, Figure 1).

VUV-PI-TOFMS. The mass spectra as a function of photon energy are shown in Figure 3 (T = 457 K), and the appearance energies (AEs) of the photoions are presented in Table 1. No signals were detected that correspond to either the ion pair (m/z 190 and 192 for $EMIM^+$ $^{79}Br^-$ and $EMIM^+$ $^{81}Br^-$, respectively) or the intact $EMIM^+$ cation (m/z 111). Also absent from the mass spectra is m/z 79, corresponding to $^{79}Br^+$, and m/z 81 is not from $^{81}Br^+$, as will be discussed below. It should be noted that the $EMIM^+$ cation has been detected on the same apparatus under similar conditions previously with the ionic liquid 1-ethyl-3-methylimidazolium bistrifluorosulfonylamide.[38]

DISCUSSION

Previous studies on aprotic imidazolium-based ionic liquids indicate their vaporization to intact C^+A^- ion pairs, based on the mass spectrometric detection of the intact cation, presumably following the dissociative ionization of the intact ion pair:

$$C^+A^- + h\nu \rightarrow C^+A + e^- \rightarrow C^+ + A\cdot + e^- \qquad (1)$$

Even though the temperatures selected for the VUV-PI-TOFMS experiments were well below the apparent onset decomposition temperature from the DSC (T_{dec} = 585 K, Figure 1), a strong photoion signal was obtained in which the signal corresponding to the cation resulting from the dissociative ionization of the ion pair ($EMIM^+$, m/z 111) was noticeably absent. However, prominent peaks at 94, 96, 108, and 110 were observed. In order to determine whether these peaks were a result of dissociative photoionization of the $EMIM^+Br^-$ ion pair, ab initio calculations were performed at the MP2/6-31+G(d,p) level of theory to calculate the AEs in the photofragmentation of the anticipated ion pair (Figure 4). It was found that, within the expected uncertainties, these AEs are calculated to occur at approximately the same AE values that occur in the experiment. However, the MP2 calculated AE for the EMIM cation at m/z 111 is 6.8 ± 0.1 eV (Figure 4) and m/z 111 is not seen experimentally, which

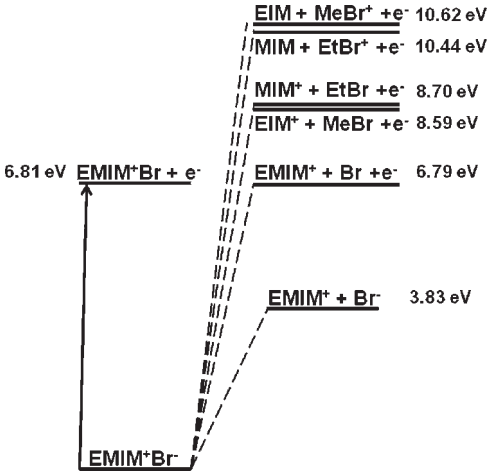

Figure 4. Energetics of the possible dissociative photoionization of $EMIM^+Br^-$. Stationary points are calculated at the MP2/6-31+G(d,p) level of theory (0 K, ZPVE corrected).

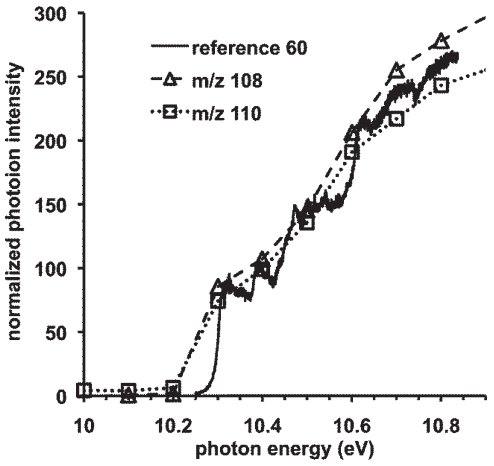

Figure 5. PIE curves for m/z 108 ($C_2H_5{}^{79}Br^+$) and m/z 110 ($C_2H_5{}^{81}Br^+$). Solid curve is total PIE data for C_2H_5Br from ref 60 (reproduced with permission of The Royal Society of Chemistry).

would suggest the presence of gaseous ion pairs to be negligible under our experimental conditions. Ultimately, by comparing not only the experimental AEs of the photoions to literature values of possible neutral species, but also their corresponding photoionization efficiency (PIE) curves to available literature PIE curves and photoelectron spectroscopy data, it is possible to identify the source of the photoions in our experiments. One beneficial aspect of the bromine system is that there are two isotopes of bromine: ^{79}Br and ^{81}Br, with natural isotope abundances of 50.69% and 49.31%, respectively. The appearance of m/z 108 and 110 with identical ion AEs and PIE curve shapes, with a 1:1 ion signal ratio would indicate that these species have a bromine atom incorporated, likely corresponding to the $C_2H_5Br^+$ ion. When our low-resolution PIE curves for m/z 108 and 110 are compared to high-resolution experimental total PIE data of ethyl bromide[60] (Figure 5), not only are the photoion AEs equal (10.3 eV), but the features of the PIE curves match as well, strongly indicating that the photoion m/z 108 and 110 originate due to the presence of ethyl bromide in the gas phase, and not from the dissociative photoionization of gaseous $EMIM^+Br^-$ ion pairs.

dx.doi.org/10.1021/jp209389d |J. Phys. Chem. A 2012, 116, 5867–5876

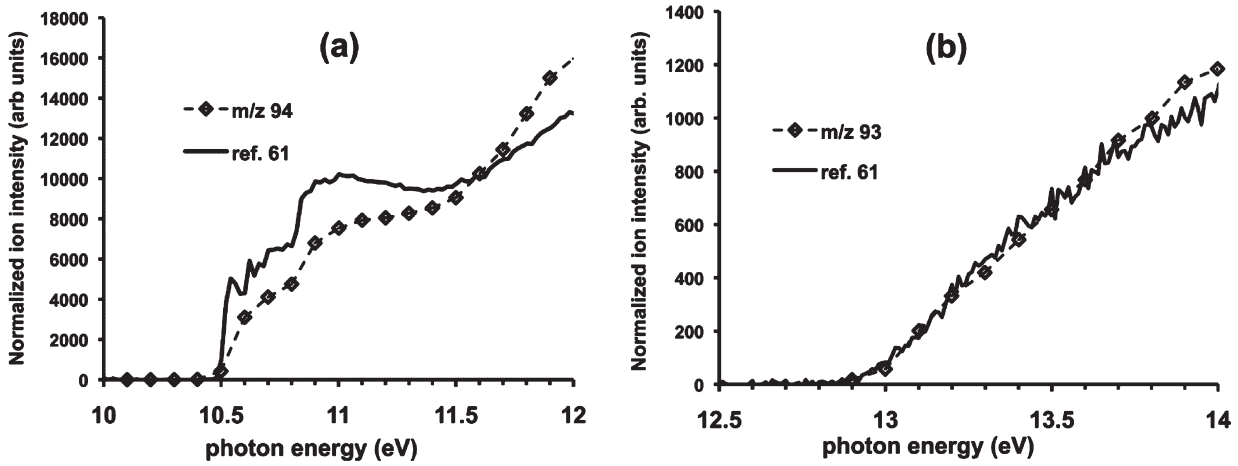

Figure 6. (a) Experimental PIE data for m/z 94 ($CH_3{}^{79}Br^+$) and (b) experimental PIE curve for m/z 93 ($CH_2{}^{79}Br^+$). Solid curves are total PIE data for CH_3Br from ref 61 (reproduced with permission from Elsevier).

A similar analysis has been performed for the possibility of generating methyl bromide from the condensed phase heating of the $EMIM^+Br^-$ ionic liquid. In this case, the corresponding masses for $CH_3{}^{79,81}Br$ would be 94 and 96. However, in Figure 3 the signal from m/z 96 is almost twice the intensity for m/z 94, and this is likely due to the contribution from two different photoions to the m/z 96 signal, $CH_3{}^{81}Br^+$ and the ethylimidazolium cation, the origin of which will be discussed below. These features are very similar to previous mass spectra generated by rapid thermolysis/mass spectrometric experiments on $EMIM^+Br^-$.[22] In comparison of the experimental PIE curve to the literature PIE of methyl bromide,[61] the AEs are equal (10.5 eV), the features of both curves match quite well (Figure 6a), and the derivative of the experimental PIE curve correlates with features in the literature photoelectron spectroscopy data[61] for CH_3Br (not shown). In addition, the PIE curves for the fragment ion, CH_2Br^+ (m/z 93 and m/z 95), have the same AEs (13.0 eV) and the curves match almost exactly (Figure 6b).

If methyl bromide and ethyl bromide are being formed by thermolysis in the heated ionic liquid, the condensed phase reactions involved would likely be

$$EMIM^+Br^- \xrightarrow{\Delta} CH_3Br + EIM \quad (2)$$

$$EMIM^+Br^- \xrightarrow{\Delta} CH_3CH_2Br + MIM \quad (3)$$

Where MIM is 1-methylimidazole (MW = 82), and EIM is 1-ethylimidazole (MW = 96). The measured AEs of photoion m/z 82 (8.6 ± 0.2 eV) and 96 (8.5 ± 0.2 eV) match well with the MP2/6-31+G(d,p) calculated ionization potentials for MIM and EIM (8.66 ± 0.1 and 8.59 ± 0.1 eV), respectively, as well as with the NIST Webbook[62] database value for MIM (8.66 eV). Assuming that the contribution from $CH_3{}^{81}Br$ to the m/z 96 PIE curve is similar in strength to the PIE for $CH_3{}^{79}Br$, the experimental EIM^+ PIE curve can be obtained simply by subtracting the PIE of m/z 94 ($CH_3{}^{79}Br$) from the observed PIE of m/z 96 (Figure 7), resulting in an experimental ionization energy for EIM of 8.5 ± 0.2 eV. From the measured AE of m/z 94 ($CH_3{}^{79}Br$), the AE of $CH_3{}^{81}Br$ of 10.5 ± 0.2 eV can be extracted (literature value for CH_3Br: IP = 10.54[63]).

The lower ion masses between m/z 40−81 are dissociative fragments mainly of EIM with a small contribution from

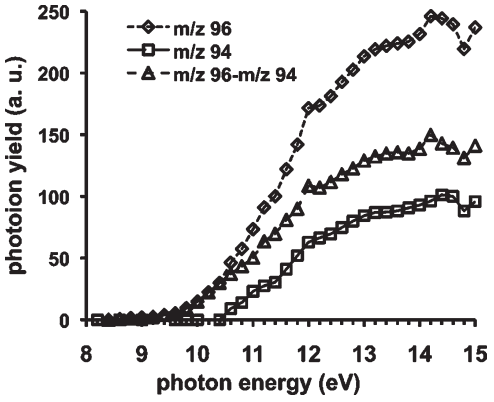

Figure 7. PIE curves for m/z 94 and m/z 96. Triangles are the difference of m/z 96 and m/z 94 PIE curves, and represent the PIE curve for EIM^+.

fragmentation of MIM, and their formation will be discussed below. Ion masses m/z 26−30 are a combination of dissociative fragments from CH_3CH_2Br, MIM, and EIM, and their formation will not be discussed here. m/z 81 (AE = 11.1 ± 0.2 eV) cannot be from $^{81}Br^+$ as a photofragment of CH_3Br or CH_3CH_2Br because not only would there be a comparable isotopic signal at m/z 79 from $^{79}Br^+$, which is not detected in Figure 3, but the $^{81}Br^+$ photoion AE from CH_3Br is greater than 15 eV.[61] Rather, the m/z 81 peak could be from either dissociative photoionization of MIM or of EIM as shown in Scheme 1.

From the M06 calculated AEs for these two photofragments, which are 11.5 ± 0.2 and 11.0 ± 0.2 eV, respectively, the experimental AE of 11.1 ± 0.2 eV indicates that m/z 81 more likely results from the EIM fragmentation channel. The relative formation of HBr (and the corresponding EMIM carbene, EMIM:) is negligible, as m/z 80 ($H^{79}Br$) is less than 1% of m/z 82 (MIM + $H^{81}Br$). This is consistent with calculations at the MP2/6-31+G(d,p) level, which show that (a) separated HBr + EMIM: is less stable than the $EMIM^+Br^-$ ion pair by 1.31 eV, and (b) proton transfer from HBr to EMIM: to form the $EMIM^+Br^-$ ion pair occurs without an energy barrier. M/z 68 (AE = 10.9 ± 0.2 eV) likely comes from EIM^+ fragmentation to form the imidazolium cation and the thermodynamically stable C_2H_4, a rather common ion fragmentation mechanism.[64] Although the calculated M06 energies (Scheme 2) for m/z 68 ion formation do

Scheme 1

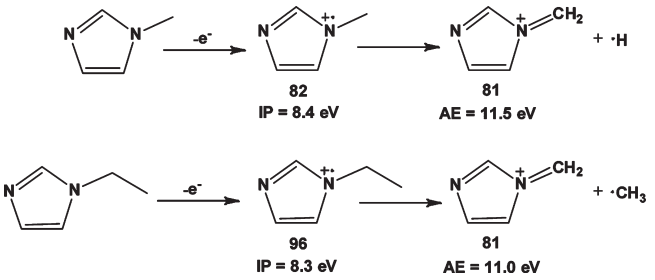

Scheme 2

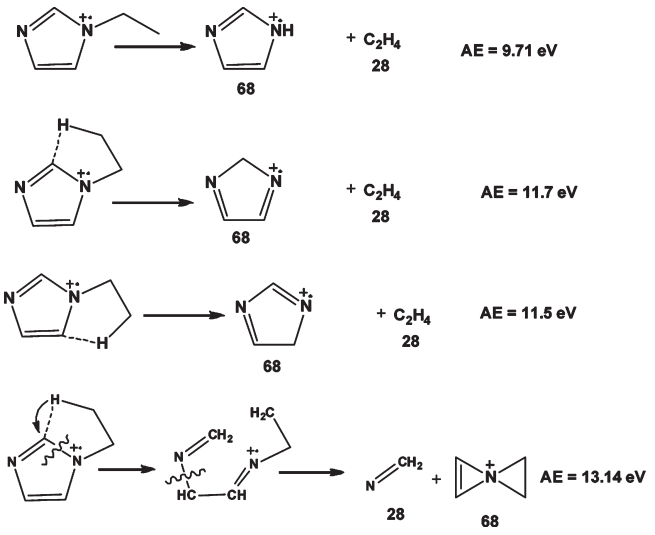

not match the experimental value exactly, the closest energy pathway is the hydrogen transfer from the terminal CH_3 group on ethyl to C4 on the imidazolium ring, followed by elimination of C_2H_4 with a calculated AE = 11.5 eV.

Another possibility is that the pathway leading to ethylene plus imidazolium ion via hydrogen transfer from the methyl group to N1 has a high barrier due to a strained geometry in the transition state, which could raise the AE above 9.7 eV. The pathway leading to formation of m/z 68 ion plus CNH_2 was also considered, but the energetics are prohibitively high for this channel (AE = 13.1 eV, Scheme 2). The formation of m/z 68 from MIM would involve the elimination of a CH_2 radical, which is highly energetically unfavorable (AE = 13.2 eV):

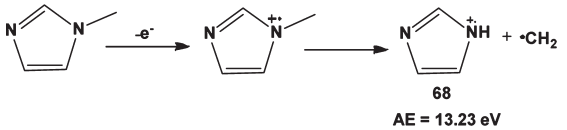

Also, from the literature, the electron impact ionization mass spectrum of EIM shows a m/z 68 fragment, whereas that of MIM does not, even at 70 eV ionization energy.[62]

Hydrogen transfer followed by ring-opening fragmentation pathways will lead to m/z 54 (AE = 11.9 ± 0.2 eV) and 42 (AE = 12.0 ± 0.2 eV). Ring-opening without hydrogen transfer would lead to ion masses not observed in the experiment. While ring-opening to form m/z 54 can only occur from EIM, m/z 42 can form from possible ring-opening of both EIM and MIM.

Scheme 3

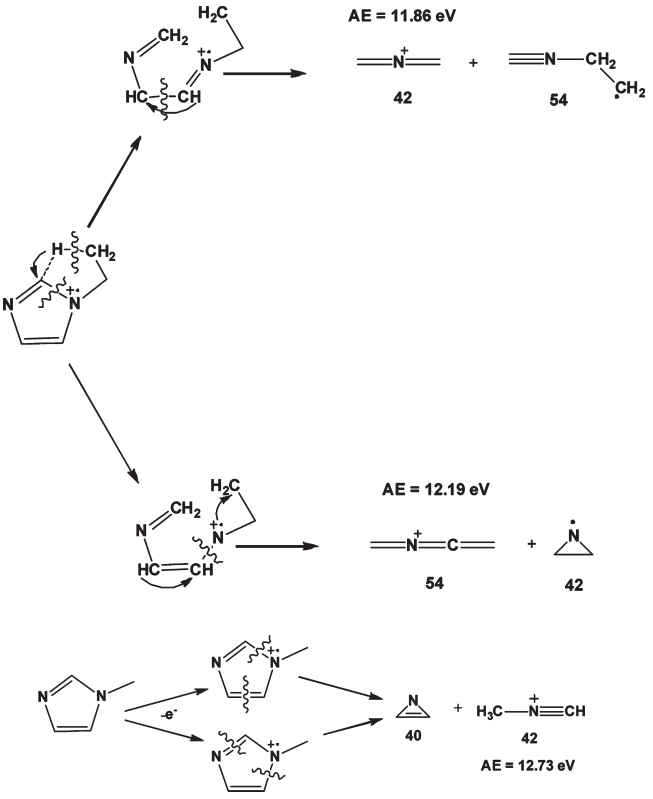

To evaluate the fragmentation of EIM^+ (m/z 96, $C_5N_2H_8$) to form m/z 42 (C_2NH_4) and m/z 54 (C_3NH_4), the enthalpies of formation of the fragments with different possible structures, both neutrals and cations, were calculated at the M06/6-31+G(d,p) level of theory. The enthalpies of formation of eight possible structures for m/z 42 and of 16 possible structures for m/z 54 were evaluated, the AEs of each combination of cation and neutral fragments were calculated, and the fragmentation pathways within ±0.5 eV of the experimental AEs were evaluated further, resulting in nine pathways in this AE range for m/z 54 cations and 26 pathways for m/z 42 cations. From this analysis, the most likely pathways were determined (Scheme 3) by matching theoretical AEs to experimental AEs and looking for the most reasonable geometries resulting from fragmentation of EIM^+. Formation of the m/z 42 and m/z 54 fragments from the EIM^+ parent must involve a hydrogen transfer followed by two ring bond cleavages. The hydrogen transfer can come from the terminal methyl group on the ethyl to the C2 position on the imidazolium ring. The calculated M06 energies are in good agreement with the experimental AEs for this pathway. m/z 42 could possibly result from fragmentation of MIM to form m/z 40 plus m/z 42 (Scheme 3). However, the calculated AE for m/z 42 is 12.7 eV, which does not match well with the experimental result for the m/z 42 AE (12.0 eV).

M/z 41 could result from MIM fragmentation involving hydrogen transfer followed by ring cleavage to form two m/z 41 fragments, and the calculated AE for the second pathway in Scheme 4 agrees very well with the experimental AE.

Assuming the rates of evaporation of CH_3Br (BP = 277 K,[62] ΔH^o_{vap} = 23.24 kJ/mol[62]) and CH_3CH_2Br (BP = 312 K,[62] ΔH^o_{vap} = 28.26 kJ/mol[62]) are much faster than the reaction rates

dx.doi.org/10.1021/jp209389d |J. Phys. Chem. A 2012, 116, 5867–5876

Scheme 4

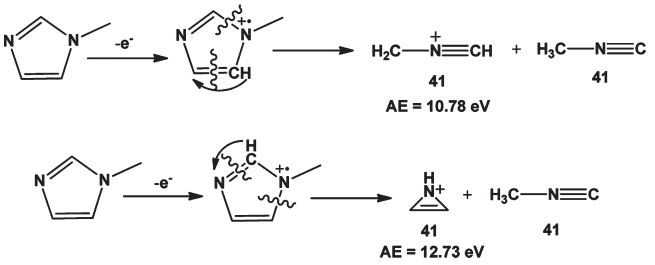

of their formation at T = 454 K through reactions 2 and 3, the branching ratio between reactions 2 and 3 above can be calculated simply by comparing the ion counts (Figure 3) for methyl bromide versus ethyl bromide. To quantify the ethyl bromide reaction, the m/z 108 and m/z 110 photoion signals were summed over all photon energies and added together. To quantify the methyl bromide reaction, the m/z 94 photoion signal was summed over all photon energies and multiplied by two in order to include the contribution from $CH_3{}^{81}Br$ (m/z 96). At T = 454 K, the calculated branching ratio for CH_3Br:C_2H_5Br is 0.76:0.24.

Previous TGA-MS/DSC studies have suggested that significant mass loss can occur well below the thermal decomposition onset temperature.[18,65] In Figure 2b, the isothermal portion of the TGA curve at T = 473 K indicates that >20% of the sample mass is lost in one hour, while the DSC does not indicate that any reaction takes place until almost 600 K. By making an Arrhenius plot with the natural log of the rate of product formation (ion signal intensity divided by temperature ramp rate, 5 K/min) versus $1/T$ (Figure 2c,d), the slope of the plot corresponds to $-\Delta H^{\ddagger}/R$ for the thermal decomposition. These activation enthalpies for m/z 94, 96, 108, and 110 yield 116.1 ± 6.6 kJ/mol and 122.9 ± 7.2 kJ/mol for reactions 2 and 3, respectively, which are consistent with the VUV-PI-TOFMS branching ratio results reported above. Uncertainties in the experimental activation enthalpies are the 95% confidence limits ($\pm 2\sigma$, precision) determined by the linear least-squares fit of the experimental data in Figures 2c and 2d. Since the activation enthalpies for thermal decomposition to CH_3Br and C_2H_5Br are almost 5 times the enthalpies of vaporization for CH_3Br and C_2H_5Br, the assumption that vaporization occurs much more rapidly than thermal decomposition seems reasonable.

Ab initio calculations were performed to determine if the reaction proceeds via a bond insertion or via an S_N2 type mechanism. Transition states for Br^- to insert into the N−C bond of the methyl and ethyl side chains were located, and their activation enthalpies were calculated. The transition states were confirmed by vibrational frequency calculations resulting in a single imaginary frequency, and IRC calculations confirmed that the products were CH_3Br + EIM (reaction 2) or CH_3CH_2Br + MIM (reaction 3). The calculated activation enthalpies via bond insertion for reactions 2 and 3 at 298 K are 239.3 and 212.1 kJ/mol, respectively (at the M06/6-31+G(d,p) level of theory). Not only are these enthalpies prohibitively high, but also reaction 3 would be favored on energetic grounds, contrary to what is observed experimentally. However, for the S_N2 reactions, the transition state enthalpies and reaction enthalpies are in good agreement with experimental results. The activation enthalpies ($\Delta H^{\ddagger}$) and enthalpies of reaction (ΔH_{rxn}, 298 K) for reactions 2 and 3 at several levels of theory can be seen in Table 2. The increased activation enthalpy for reaction 3 can be explained by steric factors, seen in Figure 8. The transition state for

Table 2. Calculated Reaction Enthalpies (298 K, kJ/mol) for Reactions 2 and 3[a]

reaction 2	activation enthalpy, $\Delta H^{\ddagger}$	ΔH_{rxn}
MP2/6-31+G(d,p)	n/a	23.1
M06/6-31+G(d,p)	134.0	15.4
CCSD(T)/6-31+G(d,p)//M06/6-31+G(d,p)	137.3	28.1
M06/aug-cc-pvtz	136.0	16.5
CCSD(T)/aug-cc-pvtz//M06/aug-cc-pvtz	130.3	21.3
reaction 3	**activation enthalpy, $\Delta H^{\ddagger}$**	**ΔH_{rxn}**
MP2/6-31+G(d,p)	n/a	24.9
M06/6-31+G(d,p)	139.0	16.2
CCSD(T)/6-31+G(d,p)//M06/6-31+G(d,p)	148.6	29.5
M06/aug-cc-pvtz	140.2	17.7
CCSD(T)/aug-cc-pvtz//M06/aug-cc-pvtz	139.9	23.1

[a] Thermal corrections obtained using unscaled harmonic vibrational frequencies.

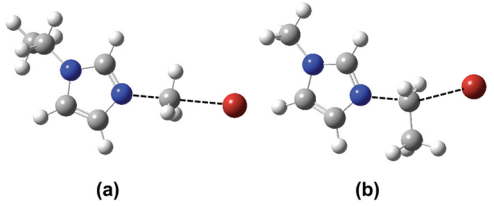

Figure 8. Transition states for the S_N2 alkyl abstraction of (a) methyl and (b) ethyl by the bromide ion at the M06/6-31+G(d,p) level of theory.

reaction 2 has a linear N−C−Br geometry with a near planar CH_3 group, and a C−Br distance of 2.55 Å at the M06/6-31+G(d,p) level of theory. The transition state for reaction 3 shows repulsion between the ethyl CH_3 group and the incoming Br^-, which causes a bend in the N−C−Br angle away from linearity, and the C−Br distance elongates to 2.65 Å, and is consistent with the presence of higher steric strain relative to the transition state for reaction 2. Increasing the basis set to aug-cc-pvtz only decreases the C−Br distance by 0.02 Å to 2.63 Å, therefore the moderate size of the 6-31+G(d,p) basis set is appropriate to accurately describe the transition state geometry for reaction 3. The decrease in magnitude of $\Delta H^{\ddagger}$ values from theory to experiment is likely due to solvent stabilization effects in the condensed phase relative to the gas phase, where the ionic liquid solvent lowers the energy of the transition state more than it does for the reactant.

To determine whether vaporization competes with thermal decomposition under vacuum distillation conditions, it is necessary to estimate the enthalpy of vaporization for $EMIM^+Br^-$. In order to estimate the enthalpy of vaporization of $EMIM^+Br^-$, several approaches were investigated. Recent work by Paulechka and co-workers[39] on the thermochemistry of the formation of 1-butyl-3-methylimidazolium bromide ($BMIM^+Br^-$) determined that the enthalpy of vaporization of $BMIM^+Br^-$ is sufficiently higher than the activation enthalpy for thermal decomposition such that saturated vapor pressure due to intact $BMIM^+Br^-$ will never be experimentally attainable. Although the enthalpy of

dx.doi.org/10.1021/jp209389d |J. Phys. Chem. A 2012, 116, 5867–5876

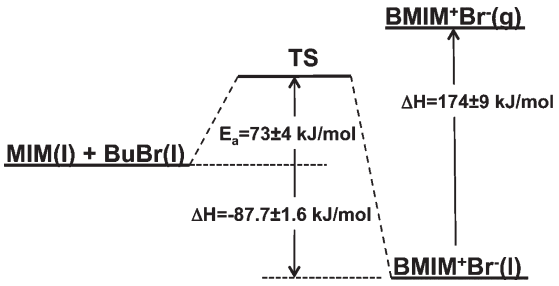

Figure 9. Energy diagram for the conversion of $BMIM^+Br^-$ to MIM + BuBr (data used with permission from ref 39).

formation of halogen-containing compounds can be calculated from the enthalpy of combustion, experimental enthalpies of combustion of halogen-containing compounds are difficult to determine accurately due to incomplete combustion and the need to accurately identify combustion products. Instead, Paulechka measured the enthalpy of reaction $MIM_{(l)} + BuBr_{(l)} \rightarrow BMIM^+Br^-_{(l)}$ calorimetrically, where BuBr is 1-butylbromide, and calculated the enthalpy of formation of the ionic liquid from this measurement using known C_p values and enthalpies of formation of MIM and BuBr. By adding the experimentally determined activation enthalpy to the enthalpy of the reaction for $MIM_{(l)} + BuBr_{(l)} \rightarrow BMIM^+Br^-_{(l)}$, the activation enthalpy for the reverse reaction (thermal decomposition) can be calculated (Figure 9). With an activation enthalpy of $\Delta H^{\ddagger} = 73 \pm 4$ kJ/mol (determined over the range of 303−334 K) and ΔH_{rxn} (298 K) = 87.7 ± 1.6 kJ/mol, the resulting activation enthalpy for the reverse reaction is 161 ± 4 kJ/mol ($\pm 2\sigma$). From the experimentally determined enthalpy of formation of $BMIM^+Br^-_{(l)}$ as well as the gas phase enthalpy of formation of the ion pair calculated by quantum chemical methods, the enthalpy of vaporization was determined to be $\Delta H_{vap}(298\ K) = 174 \pm 9$ kJ/mol. Since the estimated $\Delta H_{vap}(298\ K) = 174 \pm 9$ kJ/mol is greater than the activation enthalpy for the reverse reaction (161 ± 4 kJ/mol), on energetic grounds, thermal decomposition will dominate, and vaporization to ion pairs will not be experimentally detectable.

An alternate method for determining the enthalpy of formation in the liquid phase of the ionic liquid is to calculate the enthalpy of formation of the ion pair in the gas phase by ab initio methods (G4), and to calculate the enthalpy of vaporization of the ionic liquid using MD methods. If the enthalpy of formation of the gaseous ion pair and the enthalpy of vaporization can be calculated, the enthalpy of formation in the liquid phase of the ionic liquid can be calculated as the difference between the gas phase enthalpy of formation and the enthalpy of vaporization (see Figure 9). The gas phase enthalpies of formation $\Delta H_{f,\ gas}$(298 K) of $EMIM^+Br^-$ and $BMIM^+Br^-$ at the G4 level of theory are 38.4 ± 10 and −5.6 ± 10 kJ/mol, and the $\Delta H_{f,\ gas}$(298 K) value for $BMIM^+Br^-$ satisfactorily agrees with the literature value of $\Delta H_{f,\ gas}(298\ K) = 16 \pm 7$ kJ/mol.[39] The uncertainty of the G4 calculations for systems involving bromine were conservatively estimated at ±10 kJ/mol based on a comparison of calculated G4 enthalpies of formation of bromine containing molecules to their known literature values (Table 3). The difference in the gas phase enthalpies of formation $\Delta H_{f,\ gas}$(298 K) between $EMIM^+Br^-$ and $BMIM^+Br^-$ of 44.0 kJ/mol is consistent with the general trend of decreasing $\Delta H_{f,\ gas}$(298 K) from C_2MIM to C_4MIM observed recently.[66] Using the value of 38.4 ± 10 kJ/mol for the G4 gas phase enthalpy of formation of $EMIM^+Br^-$ and, at first

Table 3. Analysis of Uncertainties of the G4 Method for Bromine-Containing Systems[a]

	$\Delta H_{f,gas}$ G4 (298 K)	experiment[b]	uncertainty
Br^-	−215.7	−212.7	3.0
HBr	−34.1	−36.3	2.2
CH_3Br	−34.8	−34.3	0.5
CH_3CH_2Br	−62.5	−63.6	1.1

[a] Enthalpies are in kJ/mol. [b] Reference 62.

Table 4. Enthalpies of Vaporization Determined by MD Simulations.[67]

	T (K)	ΔH_{vap} (kJ/mol)
$EMIM^+Br^-$	298	147.1[b]
$EMIM^+Br^-$	393	138.3[a]
$EMIM^+Br^-$	473	130.8[a]
$BMIM^+Br^-$	298	152.8[b]
$BMIM^+Br^-$	323	150.5[a]
$BMIM^+Br^-$	393	144.0[a]

[a] MD direct calculation. [b] Linear extrapolation from higher temperature MD values.

approximation, assuming the enthalpy of vaporization of $EMIM^+Br^-$ is the same as that of $BMIM^+Br^-$ (174 ± 9 kJ/mol), the enthalpy of formation of $EMIM^+Br^-_{(l)}$ is calculated to be −136 ± 13 kJ/mol at 298 K. To improve on the accuracy of this value, MD simulations were carried out to determine the enthalpies of vaporization (ΔH_{vap}) of $EMIM^+Br^-$ and $BMIM^+Br^-$ (Table 4).[67] Enthalpies of vaporization at 298 K were determined for $EMIM^+Br^-$ and $BMIM^+Br^-$ by extrapolation from the enthalpies of vaporization determined by MD simulations at higher temperatures as indicated in Table 4. MD simulations were performed for both $EMIM^+Br^-$ and $BMIM^+Br^-$ in order to validate the ΔH_{vap} with Paulechka's experimental value for $BMIM^+Br^-$. Comparison of the ΔH_{vap}(298 K) value for $BMIM^+Br^-$ from Table 4 (152.8 kJ/mol) with the ΔH_{vap}(298 K) from Paulechka and coworkers (174 kJ/mol) indicates the MD value is low by ∼14%. Correcting for this observed systematic error would yield an estimate for $EMIM^+Br^-$ ΔH_{vap}(298 K) of 168 ± 20 kJ/mol. Using this value and the G4 gas phase enthalpy of formation of $EMIM^+Br^-$, our best estimate for the enthalpy of formation of $EMIM^+Br^-_{(l)}$ is $\Delta H_{f,\ liq}(298\ K) = -130 \pm 22$ kJ/mol. A corresponding result for $BMIM^+Br^-_{(l)}$ yields a $\Delta H_{f,\ liq}$(298 K) value of −180 ± 20 kJ/mol, which is consistent, within reported uncertainties, with that of Paulechka (−158 ± 5 kJ/mol). Similar to the findings for $BMIM^+Br^-$,[39] the ΔH_{vap}(473 K) value for $EMIM^+Br^-$ of 130.8 kJ/mol (uncorrected) is substantially larger than the experimental $\Delta H^{\ddagger}$ values for thermal decomposition (116.1 and 122.9 kJ/mol for reactions 2 and 3). Therefore, thermal decomposition effectively dominates the mass loss process for $EMIM^+Br^-$ in our experiments.

CONCLUSION

The absence of m/z 111 ($EMIM^+$ cation) from the effusive source VUV-PI-TOFMS experiment indicates that vaporization of $EMIM^+Br^-$ as intact ion pairs is not a significant pathway leading to mass loss. Instead, the observed photoions and PIE curves strongly indicate the decomposition of $EMIM^+Br^-$ to

CH_3Br, CH_3CH_2Br, MIM and EIM. TGA-MS studies and ab initio calculations support the S_N2 mechanism whereby CH_3Br formation is favored 3 to 1 over CH_3CH_2Br formation due to increased steric hindrance in the transition state for the latter path. From this work, the best estimates for the enthalpy of formation and the enthalpy of vaporization of $EMIM^+Br^-$ are $\Delta H_{f,\,liq}(298\ K) = -130 \pm 22$ kJ/mol and $\Delta H_{vap}(298\ K) = 168 \pm 20$ kJ/mol.

AUTHOR INFORMATION

Corresponding Author

*E-mail: ghanshyam.vaghjiani@edwards.af.mil; Tel: 661-275-5657; Fax: 661-275-5471.

ACKNOWLEDGMENT

The authors gratefully acknowledge funding from the U.S. Air Force Office of Scientific Research for supporting SDC and GLV (Grant No. FA9300-06-C-0023), and for CK and SRL (Grant No. FA9550-10-1-0163). This work at the ALS was supported by the Director, Office of Energy Research, Office of Basic Energy Sciences, Chemical Sciences Division of the U.S. Department of Energy under Contract No. DE-AC02-05CH11231 (A.G., O.K., and S.R.L.). We would like to thank Erik Mitchell for obtaining the DSC data, Greg Yandek and Ray Campos for the TGA data, and Wasatch Molecular Inc. for the molecular dynamics ΔH_{vap} data. This work was supported in part by a grant of computer time from the DoD High Performance Computing Modernization Program at the Air Force Research Laboratory, Army Research Laboratory, Engineer Research and Development Center, and Navy Department of Defense Supercomputing Resource Centers (DSRCs).

REFERENCES

(1) Plechkova, N. V.; Seddon, K. R. *Chem. Soc. Rev.* **2008**, *37*, 123–150.

(2) Friere, M. G.; Neves, C. M. S. S.; Marrucho, I. M.; Canongia Lopes, J. N.; Rebelo, L. P. N; Coutinho, J. A. P. *Green Chem.* **2010**, *12*, 1715–1718.

(3) Giunta, D.; Solinas, M. *Curr. Org. Chem.* **2009**, *13*, 1300–1321.

(4) Sheldon, R. *Chem. Commun.* **2001**, *23*, 2399–2407.

(5) Visser, A. E.; Swatloski, R. P.; Griffin, S. T.; Hartman, D. H.; Rogers, R. *Sep. Sci. Technol.* **2001**, *36*, 785–804.

(6) Di Noto, V.; Negro, E.; Sanchez, J.-Y.; Lojoiu, C. *J. Am. Chem. Soc.* **2010**, *132*, 2183–2195.

(7) Kim, S. Y.; Kim, S.; Park, M. J. *Nature Communications* **2010**, *1*, DOI: 10.1038/ncomms1086.

(8) Nakamoto, H.; Noda, A.; Hayamizu, K.; Hayashi, S.; Hamaguchi, H.; Watanabe, M. *J. Phys. Chem. C* **2007**, *111*, 1541–1548.

(9) Yasuda, T.; Ogawa, A.; MKanno, M.; Mori, K.; Sakakibara, K.; Watanabe, M. *Chem. Lett.* **2009**, *38*, 692–693.

(10) Armand, M.; Endres, F.; MacFarlane, D. R.; Ohno, H.; Scrosati, B. *Nat. Mater.* **2009**, *8*, 621–629.

(11) Zakeeruddin, S. M.; Graetzel, M. *Adv. Funct. Mater.* **2009**, *19*, 2187–2202.

(12) Chambreau, S. D.; Schneider, S.; Rosander, M.; Hawkins, T.; Gallegos, C. J.; Pastewait, M. F.; Vaghjiani, G. L. *J. Phys. Chem. A* **2008**, *112*, 7816–7824.

(13) Gao, H.; Joo, Y.-H.; Twamley, B.; Zhou, Z.; Shreeve, J. n. M. *Angew. Chem., Int. Ed.* **2009**, *48*, 2792–2795.

(14) Hawkins, T.; Rosander, M.; Vaghjiani, G. L.; Chambreau, S. D.; Drake, G.; Schneider, S. *Energy Fuels* **2008**, *22*, 2871–2872.

(15) Bermudez, M.-D.; Jimenez, A.-E.; Sanes, J.; Carrion, F.-J. *Molecules* **2009**, *14*, 2888–2908.

(16) Palacio, M.; Brushan, B. *Tribol. Lett.* **2010**, *40*, 247–268.

(17) Van Renesselar, J. *Tribol. Lubr. Technol.* **2010**, *66*, 24–31.

(18) Baranyai, K. J.; Deacon, G. B.; MacFarlane, D. R.; Pringle, J. M.; Scott, J. L. *Aust. J. Chem.* **2004**, *57*, 145–147.

(19) Leal, J. P.; Esperança, J. M. S. S.; Minas da Piedade, M. E.; Canongia Lopes, J. N.; Rebelo, L. P. N; Seddon, K. R. *J. Phys. Chem. A* **2007**, *111*, 6176–6182.

(20) Chan, B. K. M.; Chang, N.-H.; Grimmett, M. R. *Aust. J. Chem.* **1977**, *30*, 2005–2013.

(21) Kroon, M. C.; Buijs, W.; Peters, C. J.; Witkamp, G.-J. *Thermochim. Acta* **2007**, *465*, 40–47.

(22) Chowdhury, A.; Thynell, S. T. *Thermochim. Acta* **2006**, *443*, 159–172.

(23) Fredlake, C. P.; Crosthwaite, J. M.; Hert, D. G.; Aki, S. N. V. K.; Brennecke, J. F. *J. Chem. Eng. Data* **2004**, *49*, 954–964.

(24) Ngo, H. L.; LeCompte, K.; Hargens, L.; McEwen, A. B. *Thermochim. Acta* **2000**, *357*−*358*, 97–102.

(25) Handy, S. T.; Okello, M. *J. Org. Chem.* **2005**, *70*, 1915–1918.

(26) Breslow, R. *J. Am. Chem. Soc.* **1957**, *79*, 1962–1963.

(27) Arduengo, A. J.; Harlow, R. L.; Kline, M. *J. Am. Chem. Soc.* **1991**, *113*, 361–363.

(28) Breslow, R. *Chem. Ind.* **1957**, *26*, 893–894.

(29) Wanzlick, H. W.; Schonherr, H. J. *Liebigs Ann. Chem.* **1970**, *731*, 176–179.

(30) Kan, H.-C.; Tseng, M.-C.; Chu, Y.-H. *Tetrahedron* **2007**, *63*, 1644–1653.

(31) Holloczki, O.; Gerhard, D.; Massone, K.; Szarvas, L.; Nemeth, B.; Veszpremi, T.; Nyulaszi, L. *New J. Chem.* **2010**, *34*, 3004–3009.

(32) Koppel, I. A.; Taft, R. W.; Anvia, F.; Hu, L.-Q.; Sung, K.-S.; DesMarteau, D. D.; Yagupolskii, L. M.; Yagupolskii, Y. L.; Ignat'ev, N. V.; Kondratenko, N. V.; volkonskii, A. Y.; Vlasov, V. M.; Notario, R.; Maria, P.-C. *J. Am. Chem. Soc.* **1994**, *116*, 3047–3057.

(33) Gross, J. H. *J. Am. Soc. Mass Spectrom.* **2008**, *19*, 1347–1352.

(34) Chambreau, S. D.; Vaghjiani, G. L.; Koh, C.; Golan, A.; Strasser, D.; Leone, S. R. in preparation.

(35) Chambreau, S. D.; Vaghjiani, G. L.; To, A.; Koh, C.; Strasser, D.; Kostko, O.; Leone, S. R. *J. Phys. Chem. B* **2010**, *114*, 1361–1367.

(36) Strasser, D.; Goulay, F.; Belau, L.; Kostko, O.; Koh, C.; Chambreau, S. D.; Vaghjiani, G. L.; Ahmed, M.; Leone, S. R. *J. Phys. Chem. A* **2010**, *114*, 879–883.

(37) Strasser, D.; Goulay, F.; Kelkar, M. S.; Maginn, E. J.; Leone, S. R. *J. Phys. Chem. A* **2007**, *111*, 3191–3915.

(38) Koh, C.; Liu, C.-L.; Harmon, C.; Strasser, D.; Golan, A.; Kostko, O.; Chambreau, S. D.; Vaghjiani, G. L.; Leone, S. R. *J. Phys. Chem. A* **2011**, *115*, 4630–4635.

(39) Paulechka, Y. U.; Kabo, A. G.; Blokhin, A. V. *J. Phys. Chem. B* **2009**, *113*, 14742–14746.

(40) Becke, A. D. *J. Chem. Phys.* **1993**, *98*, 5648–5652.

(41) Hertwig, R. H.; Koch, W. *Chem. Phys. Lett.* **1997**, *268*, 345–351.

(42) Stephens, P. J.; Devlin, F. J.; Chablowski, C. F.; Frisch, M. J. *J. Phys. Chem.* **1994**, *98*, 11623–11627.

(43) Zhao, Y.; Truhlar, D. G. *Theor. Chem. Acc.* **2008**, *120*, 215–241.

(44) Clark, T.; Chandrasekhar, J.; Spitznagel, G. W.; Schleyer, P. v. R. *J. Comput. Chem.* **1983**, *4*, 294–301.

(45) Ditchfield, R.; Hehre, W. J.; Pople, J. A. *J. Chem. Phys.* **1971**, *54*, 724–728.

(46) Hariharan, P. C.; Pople, J. A. *Theoret. Chim. Acta.* **1973**, *28*, 213–222.

(47) Hehre, W. J.; Ditchfield, R.; Pople, J. A. *J. Chem. Phys.* **1972**, *56*, 2257–2261.

(48) Mitin, A. V.; Baker, J.; Pulay, P. *J. Chem. Phys.* **2003**, *118*, 7775–7782.

(49) Dunning, T. H., Jr. *J. Chem. Phys.* **1989**, *90*, 1007–1023.

(50) Wilson, A. K.; Woon, D. E.; Peterson, K. A.; Dunning, T. H. J. *J. Chem. Phys.* **1999**, *110*, 7667–7676.

(51) Gordon, M. S.; Schmidt, M. W. Advances in Electronic Structure Theory: GAMESS a Decade Later. In *Theory and Applications of Computational Chemistry: The First Forty Years*; Dykstra, C. E., Frenking, G., Kim, K. S., Scuseria, G. E., Eds.; Elsevier: Amsterdam, 2005; pp 1167−1189.

(52) Schmidt, M. W.; Baldridge, K. K.; Boatz, J. A.; Elbert, S. T.; Gordon, M. S.; Jensen, J. H.; Koseki, S.; Matsunaga, N.; Nguyen, K. A.; Su, S.; Windus, T. L.; Dupuis, M.; Montgomery, J. A. *J. Comput. Chem.* **1993**, *14*, 1347–1363.

(53) Frisch, M. J.; Trucks, G. W.; Schlegel, H. B.; Scuseria, G. E.; Robb, M. A.; Cheeseman, J. R.; Scalmani, G.; Barone, V.; Mennucci, B.; Petersson, G. A.; Nakatsuji, H.; Caricato, M.; Li, X.; Hratchian, H. P.; Izmaylov, A. F.; Bloino, J.; Zheng, G.; Sonnenberg, J. L.; Hada, M.; Ehara, M.; Toyota, K.; Fukuda, R.; Hasegawa, J.; Ishida, M.; Nakajima, T.; Honda, Y.; Kitao, O.; Nakai, H.; Vreven, T.; Montgomery, J. A., Jr. ; Peralta, J. E.; Ogliaro, F.; Bearpark, M.; Heyd, J. J.; Brothers, E.; Kudin, K. N.; Staroverov, V. N.; Kobayashi, R.; Normand, J.; Raghavachari, K.; Rendell, A.; Burant, J. C.; Iyengar, S. S.; Tomasi, J.; Cossi, M.; Rega, N.; Millam, J. M.; Klene, M.; Knox, J. E.; Cross, J. B.; Bakken, V.; Adamo, C.; Jaramillo, J.; Gomperts, R.; Stratmann, R. E.; Yazyev, O.; Austin, A. J.; Cammi, R.; Pomelli, C.; Ochterski, J. W.; Martin, R. L.; Morokuma, K.; Zakrzewski, V. G.; Voth, G. A.; Salvador, P.; Dannenberg, J. J.; Dapprich, S.; Daniels, A. D.; Farkas, Ö.; Foresman, J. B.; Ortiz, J. V.; Cioslowski, J.; Fox, D. J. *Gaussian 09*, revision A.02; Gaussian, Inc.: Wallingford, CT, 2009.

(54) Curtiss, L. A.; Redfern, P. C.; Raghavachari, K. *J. Chem. Phys.* **2007**, *126*, 084108.

(55) Borodin, O.; Smith, G. D.; Kim, H. *J. Phys. Chem. B* **2009**, *113*, 4771–4774.

(56) Innovations Through Molecular Simulations: http://www.wasatchmolecular.com/lucretiusPage.html, accessed June 11, 2011.

(57) Palmer, B. J. *J. Comput. Phys.* **1993**, *104*, 470–472.

(58) Martyna, G. J.; Tuckerman, M. E.; Tobias, D. J.; Klein, M. L. *Mol. Phys.* **1996**, *87*, 1117–1157.

(59) Paulechka, Y. U.; Kabo, G. J.; Blokhin, A. V.; Shaplov, A. S.; Lozinskaya, E. I.; Vygodskii, Y. S. *J. Chem. Thermodyn.* **2006**, *39*, 158–166.

(60) Baer, T.; Song, Y.; Liu, J.; Chen, W.; Ng, C. Y. *Faraday Discuss.* **2000**, *115*, 137–145.

(61) Locht, R.; Leyh, B.; Dahareng, D.; Hottmann, K.; Jochims, H. W.; Baumgartel, H. *Chem. Phys.* **2006**, *323*, 458–472.

(62) Afeefy, H. Y.; Liebman, J. F.; Stein, S. E. Neutral Thermochemical Data. In *NIST Chemistry WebBook, NIST Standard Reference Database Number 69*; Linstrom, P. J., Mallard, W. G., Eds.; National Institute of Standards and Technology: Gaithersburg, MD, 2005.

(63) Lias, S. G. Ionization Energy Evaluation. In *NIST Chemistry WebBook, NIST Standard Reference Database Number 69*; Linstrom, P. J., Mallard, W. G., Eds.; National Institute of Standards and Technology: Gaithersburg, MD, 2005.

(64) Yamaoka, H.; Fokkens, R. H.; Nibbering, N. M. M. *Int. J. Mass. Spectrom.* **1999**, *188*, 1–6.

(65) Arellano, I. H. J.; Guarino, J. G.; Paredes, F. U.; Arco, S. D. *J. Therm. Anal. Calorim.* **2011**, *103*, 725–730.

(66) Kabo, G. J.; Paulechka, Y. U.; Kabo, A. G.; Blokhin, A. V. *J. Chem. Thermodyn.* **2010**, *42*, 1292–1297.

(67) Bedrov, D.; Hooper, J. B. Wasach Molecular, Inc., Molecular Dynamics Determination of ΔH_{vap} of Imidazolium Bromide Ionic Liquids. Private communication.